Biochimica et Biophysica Acta 891 (1987) 265–274
Elsevier

BBA 42528

Implications of spin dynamics for the charge recombination in iron-depleted and quinone-substituted reaction centers from *Rhodobacter sphaeroides* R-26

Wilhelm Lersch and Maria Elisabeth Michel-Beyerle

Institut für Physikalische und Theoretische Chemie, Technische Universität München, Garching (F.R.G.)

(Received 20 October 1986)

Key words: Bacterial photosynthesis; Reaction center; Radical-pair decay; Magnetic-field effect; (*Rb. sphaeroides*)

Detailed calculations on the spin-dependent recombination dynamics are presented for reaction centers of *Rhodobacter sphaeroides* R-26 in which electron transfer from the primary radical pair to the iron-quinone acceptor complex has been slowed down by either iron depletion or replacement of the native ubiquinone by other quinones with different midpoint potential. Recombination yields reported for iron-depleted samples (Kirmaier, C., Holten, D., Debus, R.J., Feher, G. and Okamura, M.Y. (1986) Proc. Natl. Acad. Sci. USA 83, in the press) are compared to those in quinone-depleted reaction centers, where the forward electron transfer is completely blocked by extraction of the quinone. Within the scatter of the experimental data, the recombination pattern appears to be similar in the two different preparations indicating that the structural and kinetic features of the recombining radical pair state are not seriously affected by removal of the iron.

Introduction

In reaction centers (RCs) of the purple bacterium *Rhodobacter sphaeroides* R-26.1, the first photoinduced electron-transfer step leads within 4 ps to the formation of the transient radical-pair state P^F [1,2]. This state consists of the cation $(BChl)_2^+$ of the primary donor, the bacteriochlorophyll 'special pair' P [3,4], and the anion $BPheo^-$ of the intermediary acceptor I which has been identified with bacteriopheophytin. Under native conditions charge recombination within P^F is suppressed by rapid electron transfer from I^- to the iron-quinone complex, $Q_AFe^{2+}Q_B$, consisting of two ubiquinone molecules Q_A and Q_B with a high spin iron interposed. Electron transfer to Q_A proceeds in about 200 ps [5]. After chemical removal of the iron [6,7], this transfer was shown to slow down by a factor of approx. 50. It was also shown that in the absence of the iron recombination from P^F efficiently competes with the forward transfer to the quinone [6,7]. Depending on the spin multiplicity of the radical pair state P^F recombination either leads to the RC ground state or to the first excited triplet state P^R of the primary donor which decays to the ground state in about 24 μs in iron-depleted samples at room temperature [7].

In order to elucidate the structural and dynamical function of Fe^{2+} in the RC it is pertinent to ask, whether the drastic reduction of the forward

Abbreviations: RC(s), reaction center(s); BCHl, bacteriochlorophyll, BPheo, bacteriopheophytins, MARY, magnetic-field dependence of the reaction yield; RYDMR, reaction-yield-detected magnetic resonance.

Correspondence: M.E. Michel-Beyerle, Institut für Physikalische und Theoretische Chemie, Technische Universität München, Lichtenbergstrasse 4, 8046 Garching, F.R.G.

transfer rate in the Fe^{2+}-free case entails also changes in the dynamic and kinetic parameters characterizing the recombination from P^F. We will try to answer this question by presenting the results of quantum-mechanical calculations on the spin-dependent recombination in iron-depleted RCs and by comparing them to those obtained for quinone-depleted RCs where the forward electron transfer is completely blocked leading to 100% recombination.

A situation similar to the one in iron-depleted RCs is found in preparations where the native ubiquinone is chemically substituted by other quinones with different halfwave reduction potential $E_{1/2}$ [8]. By varying the $E_{1/2}$ value, the forward transfer rate from I^- to the quinone can be decreased by more than two orders of magnitude [8,9]. Recombination is expected to compete with the forward transfer. However, to our knowledge no recombination data exist.

For quinone-substituted as well as for iron-depleted RCs we make predictions on the form of the magnetic-field dependence of the reaction yield (MARY) and on the reaction-yield-detected magnetic resonance (RYDMR) signal, both of which having not been measured so far. Future measurements of MARY and RYDMR spectra will provide detailed information on the charge recombination in these modified RCs and may thus shed some light on the interactions emerging from Fe^{2+}. The next section gives the theoretical background of our calculations. Results are presented in the third and summarized in the last section. The Appendix gives a thorough analysis of the monoexponential decay of P^F found in both quinone-depleted and iron-depleted samples.

Theory

The spin-dependent recombination from the radical pair state P^F in quinone-depleted bacterial RCs was treated theoretically by Schulten and coworkers [10] and Haberkorn and Michel-Beyerle [11] in the framework of the stochastic Liouville equation. The forward electron transfer to Q_A in iron-depleted and quinone-substituted RCs is easily included in this equation by introducing an overall decay-rate constant k_Q describing the depopulation of P^F via electron transfer to the quinone:

$$i\hbar\frac{\mathrm{d}}{\mathrm{d}t}\rho = [\mathscr{H}, \rho] - \frac{k_S}{2}\cdot\{P^S, \rho\} - \frac{k_T}{2}\cdot\{P^T, \rho\} - k_Q\rho$$

$$= [\mathscr{H}, \rho] - \frac{k_S + k_Q}{2}\{P^S, \rho\} - \frac{k_T + k_Q}{2}\{P^T, \rho\} \tag{1}$$

$\rho(t)$ is the spin-density matrix, which describes the time evolution of the two electron and all the nuclear spins in the radical pair P^+I^-. k_S and k_T are the recombination rates from P^F to the singlet ground state and to the triplet state P^R, respectively. P^S and P^T are the projection operators to the singlet and the triplet manifold in P^F, respectively. $\{,\}$ denotes the anticommutator. The spin Hamiltonian $\mathscr{H}$ is given by

$$\mathscr{H} = g\beta[\boldsymbol{B}_0 + \boldsymbol{B}_1(t)]\cdot(\boldsymbol{S}_1 + \boldsymbol{S}_2) - JP^S + (\boldsymbol{S}_1 + \boldsymbol{S}_2)\boldsymbol{D}(\boldsymbol{S}_1 + \boldsymbol{S}_2)$$

$$+\sum_n^{(1)} A_n^{(1)}\boldsymbol{I}_n^{(1)}\boldsymbol{S}_1 + \sum_n^{(2)} A_n^{(2)}\boldsymbol{I}_n^{(1)}\boldsymbol{S}_2 \tag{2}$$

where $\boldsymbol{S}_1$, $\boldsymbol{I}_n^{(1)}$ and $\boldsymbol{S}_2$, $\boldsymbol{I}_n^{(1)}$ denote the electron spin and the nth nuclear spin on the first (P^+) and the second (I^-) radical, respectively. $\boldsymbol{B}_0$ is the static magnetic field, $\boldsymbol{B}_1(t)$ the additional microwave field in RYDMR experiments. β is Bohr's magneton, g the electron g-factor taken to be isotropic and identical for both radicals. J denotes the isotropic exchange interaction and $\boldsymbol{D}$ the dipole interaction between the electron spins on P^+ and I^-. $A_n^{(i)}$ $(i = 1, 2)$ is the isotropic hyperfine coupling constant for the nth nucleus on the ith radical. Anisotropic contributions to the hyperfine interaction were tested to play no essential role for the arguments that follow. As is evident from the second part of Eqn. 1, the treatment of the iron-depleted and the quinone-substituted cases becomes identical to the treatment of the quinone-depleted case upon replacing k_S by $k_S + k_Q$ and k_T by $k_T + k_Q$. The calculations of recombination yields, MARY and RYDMR spectra then strictly proceed along the lines detailed in Ref. 12. The orientational averages involved in the calculations with nonvanishing values of the zero-field splitting parameter D were performed as in Ref. 12, except that we assume here nonsaturating excitation con-

ditions with parallel excitation and probing transitions at an angle of 72° to the symmetry axis of the dipole tensor [13]. To avoid artefacts from the two proton model used throughout the MARY calculations, the essential results for the recombination yields were checked with a somewhat more realistic model involving nine nuclei based on a modified version [14] of the equivalence factoring method developed by Ferguson and Marquardt [15]. The results agreed within about 1% of the recombination yields.

Results and Discussion

Investigating the interplay of slow electron transfer to Q_A with recombination from P^F in iron-depleted and in quinone-substituted RCs, we start out from quinone-depleted RCs, where the forward transfer is completely blocked. We are interested in changes in the recombination pattern of P^F when the leaking electron-transfer channel to the quinone opens. In the framework of the theory outlined above, the quinone-depleted case is represented by a set of parameter values for the state P^F, which characterize the strength of the exchange (J) and the spin-dipole interaction (D) between the unpaired spins on P^+ and I^- as well as the decay rates k_S and k_T of the singlet and the triplet phased radical pair, respectively. Values for these parameters given in the literature agree more or less on the magnitude of the recombination rates k_S ($0.04 \leqslant k_S \leqslant 0.07$ ns^{-1}) and k_T ($0.3 \leqslant k_T \leqslant 0.7$ ns^{-1}), whereas there is still some discussion on the sign and the magnitude of the exchange interaction J (0.5 mT $\leqslant |J| \leqslant$ 1.6 mT) and of the zero-field splitting parameter D ($0 \leqslant |D| \leqslant 7.5$ mT) [16–20]. For the purpose of our calculations, we adopt the following set of parameter values to describe the quinone-depleted case: $k_S = 0.06$ ns^{-1}, $k_T = 0.6$ ns^{-1}, $J = -1.5$ mT, $D = -1.1$ mT, $E = 0$ mT. Except for $D = -1.1$ mT these values were used in Ref. 12 to interpret the RYDMR data from Ref. 17. The zero-field splitting $D = -1.1$ mT in the radical pair $(BChl)_2^+$ $BPheo^-$ was calculated from the X-ray structure of *Rhodopseudomonas viridis* [13,21]. This low value for D contrasts to the conclusions drawn by other groups from MARY and RYDMR experiments [17,18]. (Up to now it is not clear whether this discrepancy is due to a spread in sample properties or to experimental artefacts as those caused by saturating light intensities and high microwave powers [20].) The hyperfine interaction in the two radicals is modelled either by two representative nuclei with coupling constants $A_1 = 0.95$ mT and $A_2 = 1.3$ mT [18] (calculation of MARY data) or by Gaussian distributions of the hyperfine fields with second moments 'A_1' = 0.95 mT and 'A_2' = 1.3 mT, respectively (calculation of RYDMR spectra). All calculations refer to times shorter than 1 μs after creation of the radicals in order to avoid additional complicaitons by the postulated repopulation of P^F from P^R [22].

We now make the assumption that on slowly switching on the forward transfer to the quinone, the recombination dynamics remain essentially unaltered. If this holds true, we can describe the iron-depleted and the quinone-substituted cases by just adding an overall decay rate constant k_Q to the spin-selective rates k_S and k_T (see Theory). By doing so, we obtain the MARY and RYDMR spectra shown in Fig. 1. The forward rate k_Q is varied in the range 0.05–0.5 ns^{-1}, typical for some substituted quinones (Refs. 8 and 9; see also Dutton, P.L., personal communication) and for iron-depleted RCs, where $k_Q \approx 0.1$ ns^{-1} [7]. The corresponding lifetimes of P^F and the recombination yields are given in Table I. As one would expect, the singlet and the triplet recombination yields (ϕ_S and ϕ_T) decrease upon increasing the leakage rate k_Q to the quinone. The magnetic field effect on the recombination yields diminishes and the MARY spectra become very broad due to the shortening of the P^F lifetime. Most striking is the sensitivity of the RYDMR spectrum to the value of k_Q (i.e., to the lifetime of P^F) for a microwave field strength $B_1 \approx |J|$ (Fig. 1B). A similar sensitivity was observed in a different situation, where the radical spins undergo a hopping process between two or many different sites [23]. This feature of RYDMR spectra is due to microwave-induced singlet–triplet level crossing in the rotating frame, the influence of decay rates on the triplet recombination yield being most pronounced at the crossing point.

To our knowledge no MARY or RYDMR spectra exist for iron-depleted or quinone-substituted RC preparations. Future measurements

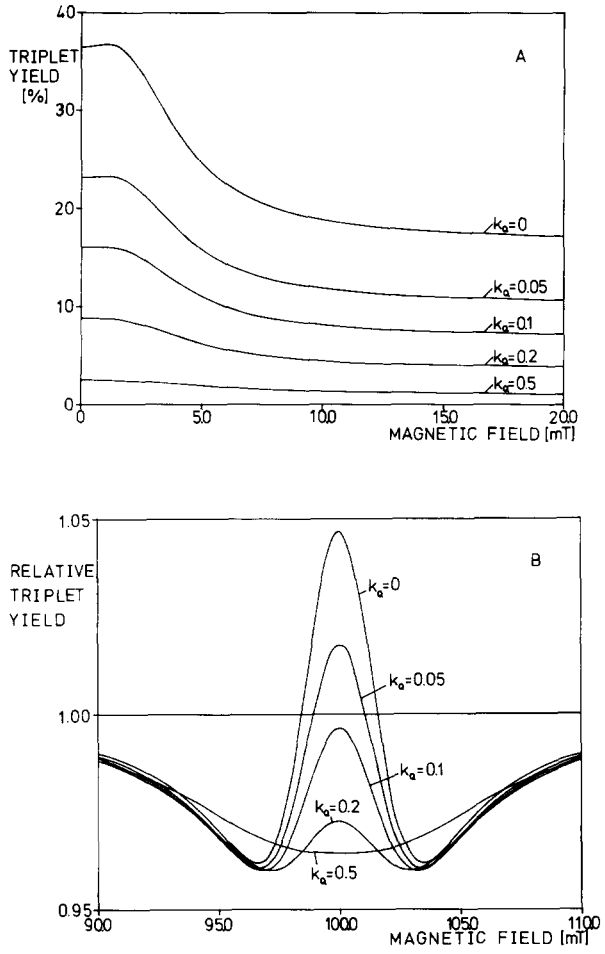

Fig. 1. (A) MARY and (B) RYDMR spectra for different values of the forward transfer rate k_Q. k_Q is indicated in ns^{-1}. Other parameters: $A_1 = 0.95$ mT, $A_2 = 1.3$ mT, $J = -1.5$ mT, $D = -1.1$ mT, $E = 0$ mT, $k_S = 0.06$ ns^{-1}, $k_T = 0.6$ ns^{-1}, $t = 30$ ns, $B_1 = 1.3$ mT (RYDMR spectra). The relative triplet yield in the RYDMR spectra is defined as $\phi_T(B_0, B_1, t)/\phi_T(B_0, 0, t)$.

will be compared to the predictions in Fig. 1 to see what changes occur in the recombination dynamics in addition to the depopulation of P^F via k_Q. In the case of iron-depleted RCs experimental data exist on the lifetime of P^F and on the recombination yields [7]. P^F was found to decay monoexponentially with a lifetime τ_{P^F} of 4.2 ± 0.3 ns yielding the singlet ground state ($28 \pm 5\%$), the triplet state P^R ($25 \pm 5\%$) and the charge-separated state $P^+IQ_A^-$ ($47 \pm 5\%$) [7]. As shown in the Appendix, the single exponential decay of P^F

TABLE I

CALCULATED RECOMBINATION YIELDS AND P^F LIFETIMES FOR DIFFERENT FORWARD TRANSFER RATES k_Q TO THE QUINONE

2 proton model, $B_0 = 0$ mT, $A_1 = 0.95$ mT, $A_2 = 1.3$ mT, $J = -1.5$ mT, $D = -1.1$ mT, $E = 0$ mT, $k_S = 0.06$ ns^{-1}, $k_T = 0.6$ ns^{-1}, $t = 500$ ns. $\tau_{P^F}^{1/e}$ is the time where P^F has decayed to $1/e$ of its initial value ($= 1$).

k_Q (ns^{-1})	$\tau_{P^F}^{1/e}$ (ns)	ϕ_S	ϕ_T	ϕ_Q
0	10.6	0.61	0.39	0
0.01	9.7	0.55	0.35	0.10
0.05	7.2	0.40	0.24	0.36
0.1	5.4	0.30	0.16	0.54
0.2	3.6	0.20	0.09	0.71
0.5	1.8	0.10	0.03	0.87
1.0	1.0	0.06	0.01	0.93

justifies to estimate k_S and k_Q from the respective yields ($\phi_S \approx k_S \tau_{P^F}$, $\phi_Q \approx k_Q \tau_{P^F}$). This gives a value of $k_S \approx 0.07$ ns^{-1} and of $k_Q \approx 0.11$ ns^{-1}. k_S seems to have not much changed compared to quinone-depleted RCs. To see whether the same is true for the other parameters k_T, J and D, we calculated τ_{P^F}, ϕ_S, ϕ_T and ϕ_Q using the parameter values for the quinone-depleted case and the above value for k_Q. We get $\tau_{P^F}^{1/e} = 5.2$ ns, $\phi_S = 0.29$, $\phi_T = 0.15$ and $\phi_Q = 0.56$ (Table II). The agreement of these calculated values with the experimental results is not very satisfactory. The P^F lifetime $\tau_{P^F}^{1/e}$, calculated as the time where P^F has decayed to $1/e$ of its initial value ($= 1$), is somewhat longer than the measured value of $\tau_{P^F} = 4.2 \pm 0.3$ ns. However, as will be discussed later, the theoretical decay curves for P^F deviate from monoexponentiality at early times (Fig. 2) such that $\tau_{P^F}^{1/e}$ is longer than the decay time τ_{P^F} one obtains by approximating the theoretical curve by a single exponential. τ_{P^F} equals 4.8 ns in the present case. This is still slightly above the experimental value. Moreover, the calculated triplet yield is smaller than the experimental one, whereas the yield ϕ_Q of the charge-separated state $P^+IQ_A^-$ comes out too large. This means that we either chose the wrong parameter set to describe the quinone-depleted case or that some of the parameters have changed on going over from the quinone-depleted to the iron-depleted case. To cover both possibilities, we show

TABLE II

RECOMBINATION YIELDS AND P^F LIFETIME IN IRON-DEPLETED RCs CALCULATED WITH DIFFERENT SETS OF THE PARAMETERS k_S, k_T, J AND D

2 proton model, $A_1 = 0.95$ mT, $A_2 = 1.3$ mT, $E = 0$ mT, $k_Q = 0.11$ ns^{-1}, $B_- = 0$ mT, $t = 500$ ns. $\tau_{P^F}^{1/e}$ is calculated as the time where P^F has decayed to $1/e$ of its initial value ($=1$) at $t = 0$ ns.

D (mT)	J (mT)	k_S (ns^{-1})	k_T (ns^{-1})	$\tau_{P^F}^{1/e}$ (ns)	ϕ_S	ϕ_T	ϕ_Q
−1.1	−1.5	0.06	0.2	5.5	0.29	0.12	0.59
			0.4	5.3	0.29	0.15	0.56
			0.6	5.2	0.29	0.15	0.56
			0.8	5.1	0.29	0.15	0.56
			1.0	5.1	0.30	0.15	0.55
−1.1	−1.5	0.02	0.6	6.3	0.12	0.19	0.69
		0.04		5.7	0.21	0.17	0.62
		0.06		5.2	0.29	0.15	0.56
		0.08		4.7	0.35	0.14	0.51
		0.10		4.4	0.40	0.13	0.47
−1.1	2.0	0.06	0.6	5.1	0.28	0.17	0.55
	1.0			5.1	0.27	0.20	0.53
	0.0			5.1	0.27	0.20	0.53
	−1.0			5.1	0.28	0.17	0.55
	−2.0			5.2	0.30	0.13	0.57
−6.0	−1.5	0.06	0.6	5.3	0.31	0.10	0.59
−3.0				5.2	0.29	0.14	0.57
0.0				5.2	0.29	0.15	0.56
3.0				5.2	0.29	0.16	0.55
6.0				5.2	0.29	0.16	0.55
0	0.4	0.06	0.2	5.4	0.24	0.20	0.56
			0.4	5.2	0.25	0.22	0.53
			0.6	5.1	0.27	0.21	0.52
			0.8	5.1	0.28	0.19	0.53
			1.0	5.1	0.28	0.18	0.54
0	0.4	0.02	0.6	6.1	0.11	0.26	0.63
		0.04		5.5	0.19	0.23	0.58
		0.06		5.1	0.27	0.21	0.52
		0.08		4.7	0.33	0.19	0.48
		0.10		4.3	0.38	0.17	0.45
0	2.0	0.06	0.6	5.1	0.28	0.17	0.55
	1.0			5.1	0.27	0.20	0.53
	0.0			5.1	0.27	0.21	0.52
	−1.0			5.1	0.28	0.18	0.54
−6.0	0.4	0.06	0.6	5.2	0.30	0.14	0.56
−3.0				5.1	0.28	0.18	0.54
0.0				5.1	0.27	0.21	0.52
3.0				5.1	0.28	0.18	0.54
6.0				5.2	0.30	0.13	0.57

in Table II how the results for $\tau_{P^F}^{1/e}$, ϕ_S, ϕ_T, and ϕ_Q depend on the variables k_S, k_T, J and D. Pursuing the latter possibility of a structural change in the RC, we note that, in order to obtain nearly equal singlet and triplet recombination yields, the singlet–triplet mixing efficiency must have increased compared to the quinone-depleted preparations. This implies that the energy gap between the singlet and the triplet manifold has decreased. Table II shows that the highest triplet yield is obtained for $J \approx 0$, $D \approx 0$, a situation where singlet and triplet states are nearly degenerate in zero-magnetic field. In fact, our best simulations of the recombination data of Ref. 7 gave parameter values around $k_Q = 0.11$ ns^{-1}, $k_S = 0.06$ ns^{-1}, $k_T = 0.6$ ns^{-1}, $J = 0.4$ mT, $D = 0$ mT (Table II). With these values and with $A_1 = 0.95$ mT and $A_2 = 1.3$ mT we calculated $\tau_{P^F}^{1/e} = 5.1$ ns ($\tau_{P^F} = 4.3$ ns), $\phi_S = 0.27$, $\phi_T = 0.21$ and $\phi_Q = 0.52$ in close agreement with the experimental results. In contrast to the findings of Ref. 7, however, we do not obtain a strictly monoexponential decay of P^F (Fig. 2 and Appendix), which manifests itself in the deviation of the $1/e$-time $\tau_{P^F}^{1/e}$ from the decay time τ_{P^F} of the exponential approximation to the theoretical curve. This is true for quinone-depleted RCs (Fig. 2, curve a), but becomes more pronounced in the simulations of the P^F decay in iron-depleted samples (Fig. 2, curves b and c). Minimization of the singlet–triplet energy gap to obtain the high triplet to singlet yield ratio found in these preparations strengthens the nonexponential behaviour of the p^F decay. This is illustrated in Fig. 2, where curve b ($J = -1$ mT) deviates less from exponential than curve c ($J = 0.4$ mT), but reproduces worse the recombination yields, which are $\phi_S = 0.28$, $\phi_T = 0.18$, $\phi_Q = 0.54$ for curve b and $\phi_S = 0.27$, $\phi_T = 0.21$, $\phi_Q = 0.52$ for curve c, respectively (experimental $\phi_S = 0.28 \pm 0.05$, $\phi_T = 0.25 \pm 0.05$, $\phi_Q = 0.47 \pm 0.05$ [7]). Presumably, the nonexponential behaviour predicted by our calculations is difficult to detect and was beyond the experimental resolution in Ref. 7. Nevertheless, one should be careful about analyzing the recombination dynamics in purely exponential terms instead of applying the full quantum-mechanical description.

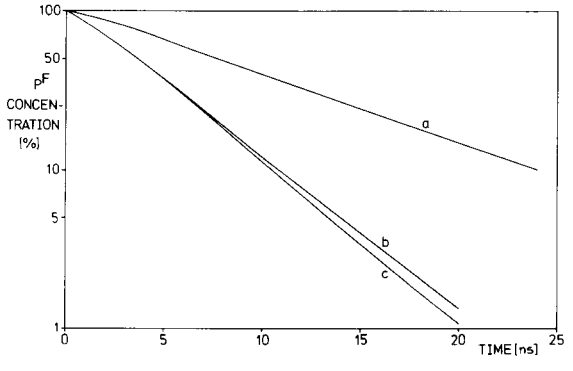

Fig. 2. P^F decay calculated for quinone-depleted (a) and iron-depleted (b, c) RCs, respectively. Parameters: $A_1 = 0.95$ mT; $A_2 = 1.3$ mT; $J = -1.5$ mT (a), -1.0 mT (b), 0.4 mT (c); $D = -1.1$ mT (a), 0 mT (b, c); $E = 0$ mT; $k_S = 0.06$ ns^{-1}; $k_T = 0.6$ ns^{-1}; $k_Q = 0$ ns^{-1} (a), 0.11 ns^{-1} (b, c); $B_0 = 0$ mT. (Using $D = -1.1$ mT also in the iron-depleted case has almost no influence on curves b and c.)

Comparing the parameters used to model the recombination dynamics in iron-depleted RCs with those for quinone-depleted preparations, the exchange interaction J seems to have changed noticeably, the other parameters more or less retaining their values. One has to be careful about this conclusion, however. The value of $|J| = 1.5$ mT adopted in our description of the quinone-depleted case strongly depends on the sign and the shape of the RYDMR spectrum. Recent measurements of the RYDMR signal at low microwave powers give evidence for a value of $|J|$ lower than 1.5 mT in quinone-depleted samples [19]. A lower value of $|J|$ was also found in former, time-resolved MARY-measurements on quinone-depleted RCs [16] which exhibited a singlet-to-triplet recombination yield ratio close to the one obtained in Ref. 7 for the iron-depleted case. Moreover, the P^F lifetime and the zero-field recombination yields at long times after the creation of the radicals by themselves are not very sensitive to the values of k_T, J and D (Table II). To decide really whether these parameters do change or don't, consistent sets of MARY and RYDMR data are needed for iron-depleted as well as for quinone-depleted preparations. k_S and k_Q, however, can be obtained quite accurately from the exponential lifetime of P^F and the corresponding yields (Tables I and II).

Conclusions

Starting from the situation found in quinone-depleted RCs, where 100% of the initially created radical pairs recombine, we made predictions on the shape of MARY and RYDMR spectra and on the recombination yields in iron-depleted and quinone-substituted RCs, where part of the radicals escape recombination to form the charge-separated state $P^+IQ_A^-$. Comparison of these predictions with experimental data on the charge recombination from P^F in the iron-depleted case [7] is hampered by the uncertainty of the measured recombination yields in the quinone-depleted case and the concomitant scatter of the parameter values used in the literature to describe the quinone-free situation [16–20]. Clearly, a more exact definition is needed on what one has to understand as the 'quinone-depleted case' (including sample preparation, aging and experimental conditions such as illumination intensity) in order to have a reliable standard to compare with other RC preparations. To this end highly accurate MARY measurements are in progress.

The apparent monoexponential decay of P^F in iron-depleted samples was shown to allow a reasonable estimate of the singlet recombination rate k_S and the forward transfer rate k_Q (but not the triplet recombination rate k_T) from the respective yields. The value of $k_S = 0.07\ ns^{-1}$, which also comes out from our quantum-mechanical calculations, agrees with the value obtained in Ref. 17 for the quinone-depleted case. The value of $k_Q = 0.11\ ns^{-1}$ confirms the conclusion of Ref. 7 that the forward transfer rate to Q_A in iron-depleted RCs is slowed down by a factor of approx. 50 compared to the native case. Decisive conclusions on changes of k_T, the exchange interaction J and the zero-field splitting parameter D in the radical pair state P^F require consistent information from MARY and RYDMR experiments on iron-depleted as well as on quinone-depleted samples.

After completion of this work two related publications appeared dealing with the $E_{1/2}$ dependence of the forward electron transfer $P^+I^-Q_A \rightarrow P^+IQ_A^-$ and of the back reaction $P^+IQ_A^- \rightarrow PIQ_A$ in quinone-substituted RCs [24,25]. The quantum yield of the charge-separated state $P^+IQ_A^-$ is found to be substantially lower than 100% in preparations, where the native ubiquinone is replaced by different low-potential anthraquinones, indicating a high percentage of recombination from P^F. 2,3-Dimethylanthraquinone with a quantum yield $\phi_Q = 0.45$ [24] seems to be an attractive candidate for the MARY and RYDMR experiments proposed in the present communication.

Appendix

Iron-depleted RCs show a monoexponential decay of P^F with a time constant $\tau_{P^F} = 4.2 \pm 0.3$ ns [7]. A single exponential decay of P^F is also found in quinone-depleted RCs [18,26]. We want to comment on the question whether the monoexponentiality of the overall decay of P^F justifies a first-order rate constant description for the decay of P^F through the singlet, the triplet and the quinone channel. Such a description was adopted in Refs. 6 and 7, and we will see how the rate constants k_S, k_T and k_{IQ} used there are related to the rate constants of our quantum-mechanical description in Eqn. 1. For our arguments we use analytical expressions for the time-dependent $P_F(t)$ population which were derived in Ref. 27 and published by part in Ref. 28. At high static magnetic field strengths ($B_0 \gtrsim 0.1$ T) the singlet and the triplet content of P^F, p_S and p_T, are given by Refs. 27 and 28:

$$p_S(t) = \frac{1}{N}\sum_{k=1}^{N}\Big\{\left(1+2\Lambda'_k+|\Lambda_k|^2\right)e^{-2E''_{1,k}t}+|\Lambda_k|^2\,e^{-2E''_{2,k}t} +2\left[\Lambda''_k\sin\Omega'_k t-\left(\Lambda'_k+|\Lambda_k|^2\right)\cos\Omega'_k t\right] \times e^{-(E''_{1,k}+E''_{2,k})t}\Big\} \tag{A-1}$$

and

$$p_T(t) = \frac{1}{N}\sum_{k=1}^{N}\frac{a_k^2}{|\Omega_k|^2}\left(e^{-2E''_{1,k}t}+e^{-2E''_{2,k}t} -2\cos\Omega'_k t\,e^{-(E''_{1,k}+E''_{2,k})t}\right) \tag{A-2}$$

respectively. The index k runs over all N possible configurations of the nuclear spins in the two radicals. The two eigenvalues $E_{1,k}$ and $E_{2,k}$ of the high-field Hamiltonian are given by (primed quan-

tities are real):

$$E_{(2)}^{1,k} = E_{(2)}^{1,k\prime} - iE_{(2)}^{1,k\prime\prime} = -\frac{1}{2}\left[J + D_{zz} + i\frac{k_S + k_T + 2k_Q}{2}\right] \pm_{(-)} \frac{1}{2}\sqrt{(2a_k)^2 + \left(-J + D_{zz} + i\frac{k_T - k_S}{2}\right)^2} \quad \text{(A-3)}$$

where $D_{zz} = z\boldsymbol{D}z$ and $a_k = \frac{1}{2}(\beta B_0 \Delta g_{zz} + \sum_n^{(1)} A_n^{(1)} m_{n,k}^{(1)} - \sum_n^{(2)} A_n^{(2)} m_{n,k}^{(2)})$. Δg_{zz} is the component of the difference g-tensor in the magnetic-field ($= z$-) direction; $m_{n,k}$ is the z-projection of the nth nuclear spin in the kth spin configuration. $\Omega_k = \Omega_k' - i\Omega_k''$ denotes the energy difference $\Omega_k = E_{1,k} - E_{2,k}$. $\Lambda_k = \Lambda_k' + i\Lambda_k''$ is given by

$$\Lambda_k = \frac{1}{2}\left[\frac{-J + D_{zz} + i\frac{k_T - k_S}{2}}{\Omega_k} - 1\right] \quad \text{(A-4)}$$

in the high-field case.

In the zero-field case expressions closely resembling those in Eqns. A-1 and A-2 can be derived in the framework of the one-proton model [11,27]. We get [27]:

$$p_S(t) = (1 + 2\lambda' + |\lambda|^2)\, e^{-2\varepsilon_1'' t} + |\lambda|^2 e^{-2\varepsilon_2'' t} + 2[\lambda'' \sin \omega' t - (\lambda' + |\lambda|^2)\cos \omega' t]\, e^{-(\varepsilon_1'' + \varepsilon_2'')t} \quad \text{(A-5)}$$

and

$$p_T(t) = 3\frac{(A/4)^2}{|\omega|^2}\left(e^{-2\varepsilon_1'' t} + e^{-2\varepsilon_2'' t} - 2\cos \omega' t\, e^{-(\varepsilon_1'' + \varepsilon_2'')t}\right) \quad \text{(A-6)}$$

The eigenenergies $\varepsilon_1 = \varepsilon_1' - i\varepsilon_1''$ and $\varepsilon_2 = \varepsilon_2' - i\varepsilon_2''$ are now given by:

$$\varepsilon_{(2)}^{1} = -\frac{1}{2}\left(J + \frac{A}{2} + i\frac{k_T + k_S + 2k_Q}{2}\right) \pm_{(-)} \frac{1}{2}\sqrt{3\left(\frac{A}{2}\right)^2 + \left(-J + \frac{A}{2} + i\frac{k_T - k_S}{2}\right)^2} \quad \text{(A-7)}$$

where A is the hyperfine coupling constant of the single proton considered. The dipole interaction cannot be taken into account in this case. $\omega = \omega' - i\omega''$ denotes the energy difference $\omega = \varepsilon_1 - \varepsilon_2$. $\lambda = \lambda' + i\lambda''$ now takes the form

$$\lambda = \frac{1}{2}\left[\frac{-J + \frac{A}{2} + i\frac{k_T - k_S}{2}}{\omega} - 1\right] \quad \text{(A-8)}$$

Inspection of Eqns. A-1, A-2 and A-5, A-6 shows that the decay of P^F is not monoexponential in the general case. In order to explain the experimental results, we therefore consider two special cases where the quantum-mechanical description in fact gives nearly single exponential behaviour for the P^F decay. These are (i) $E_{2,k}'' \gg E_{1,k}''$ ($\varepsilon_2'' \gg \varepsilon_1''$) and (ii) $|\Lambda_k| \ll 1$ ($|\lambda| \ll 1$). (A strictly single exponential decay is obtained for $k_S = k_T$. We do not pursue this possibility, however, as it can be ruled out from an analysis of the measured recombination yields. For the same reason, we disregard the case $k_Q \gg k_S$, k_T.)

Case (i) is realized for large values of k_T compared to k_S and the hyperfine interaction. It is the only case where the formation of triplets can be approximately described by a first-order rate-constant decay from P^F ($t \gg 1/(2E_{2,k}'')$, $1/(2\varepsilon_2'')$): $\mathrm{d}/\mathrm{d}t(\phi_T)_k \approx k_T a_k^2/|\Omega_k|^2 p_F$ ($\mathrm{d}/\mathrm{d}t\ \phi_T \approx k_T \cdot 3(A/4)^2/|\omega|^2 p_F$), where $p_F \approx \exp(-2E_{1,k}'' t)$ ($p_F \approx \exp(-2\varepsilon_1'' t)$. In this case the rate constants 'k_S' and 'k_{IQ}' from Refs. 6 and 7 agree with our rate constants k_S and k_Q, whereas their k_T is given by $k_T a_k^2/|\Omega_k|^2$ ($k_T \cdot 3(A/4)^2/|\omega|^2$) in our high-field (zero-field) terminology. Calculating $\varepsilon_1''/\varepsilon_2''$ for the values of k_S, k_T, $A = \sqrt{A_1^2 + A_2^2}$ and J specified in the text we get a value of 0.16 for quinone-depleted and a value of 0.48 for iron-depleted RCs at zero field. These values should be considered as order-of-magnitude estimates. Nevertheless, they indicate that case (i) is probably not realized in these RC preparations.

Case (ii) also gives a quasi-exponential decay of P^F subject to the weaker condition $|\Lambda_k| \ll 1$ ($|\lambda| < 1$) which is equivalent to I hyperfine interaction complex singlet–triplet energy difference $I^2 = a_k^2/\{(J - D_{zz})^2 + (k_T - k_S)^2/4\} \ll 1$ [$3(A/4)^2/\{(-J + A/2)^2 + (k_T - k_S)^2/4\} \ll 1$]. Similar to case (i) the radical pair state P^F is predominantly singlet-phased and (apart from very early times) decays monoexponentially with the time

constant $(\tau_{P^F})_k = 1/(2E''_{1,k})$ $[\tau_{P^F} = 1/(2\varepsilon''_1)]$. The singlet yield and the yield of the charge separated state $P^+IQ_A^-$ are given by $\phi_S \approx k_S\tau_{P^F}$ and $\phi_Q \approx k_Q\tau_{P^F}$, respectively, the rate constants k_S and k_Q being identical with 'k_S' and 'k_{IQ}' from Refs. 6 and 7. In contrast to case (i), however, the depopulation of P^F through the triplet channel cannot be described by a first-order rate constant, since all the three exponentials in Eqns. A-2 and A-6 are now equally important. This implies that the rate constant 'k_T' from Refs. 6 and 7 which is defined by $\phi_T = k_T\tau_{P^F}$ is not easily related to the parameters of the time-dependent quantum-mechanical description in this case. Calculating $|\lambda|$, we obtain a value of 0.06 for quinone-depleted and a value of 0.32 for iron-depleted RCs at zero field. This means that case (ii) represents a better approximation for the situation met in quinone-depleted RCs than case (i) which imposes more stringent conditions on the triplet lifetime compared to the overall lifetime of P^F ($k_T\tau_{P^F} \gg 1$). Iron-depleted samples, however, seem to be as badly characterized by case (ii) as they are by case (i), such that we would not expect to obtain a monoexponential decay for them. We are aware of the fact that the one-proton model underlying our arguments in the zero-field situation somewhat overestimates the deviation from monoexponentiality as it takes into account only one large hyperfine coupling. Therefore, the decay curves shown in Fig. 2 were calculated with models involving up to nine nuclei. Nevertheless, these numerical results support the conclusion from the above analytical arguments that decrease the singlet–triplet energy gap to obtain higher triplet-to-singlet yield ratios means strengthen the nonexponentiality of the P^F decay.

Acknowledgements

We are highly indebted to Prof. G. Feher for stimulating this work and for sending us a preprint of Ref. 7. We are also very grateful to Dr. Dutton for providing us with data on the forward transfer rates in quinone-substituted RCs and to Dr. M. Gunner for a preprint of Ref. 25. Financial support by the Deutsche Forschungsgemeinschaft (SFB 143) is gratefully acknowledged.

References

1 Martin, J.L., Breton, J., Hoff, A.J., Migus, A. and Antonetti, A. (1986) Proc. Natl. Acad. Sci. USA 83, 957–961
2 Woodbury, N.W., Becker, M., Middendorf, D.V. and Parson, W.W. (1986) Biochemistry 24, 7516–7521
3 Norris, J.R., Uphaus, R.A., Crespi, H.L. and Katz, J.J. (1971) Proc. Natl. Acad. Sci. USA 68, 625–628
4 Feher, G., Hoff, A.J., Isaacson, R.A. and Ackerson, L.C. (1975) Ann. NY Acad. Sci. 244, 239–259
5 Parson, W.W. and Ke, B. (1982) in Photosynthesis: Energy Conversion by Plants and Bacteria (Govindjee, ed.), pp. 331–385, Academic Press, New York
6 Debus, R.J., Feher, G. and Okamura, M.Y. (1986) Biochemistry 25, 2276–2287
7 Kirmaier, C., Holten, D., Debus, R.J., Feher, G. and Okamura, M.Y. (1986) Proc. Natl. Acad. Sci. USA 83, in the press
8 Gunner, M.R., Tiede, D.M., Prince, R.C. and Dutton, P.L. (1982) in Function of Quinones in Energy Conserving Systems (Trumpower, B.L., ed.), pp. 265–269, Academic Press, New York
9 Liang, Y., Negus, D.K., Hochstrasser, R.M., Gunner, M.R. and Dutton, P.L. (1981) Chem. Phys. Lett. 84, 236–240
10 Werner, H.-J., Schulten, K. and Weller, A. (1978) Biochim. Biophys. Acta 502, 255–268
11 Haberkorn, R. and Michel-Beyerle, M.E. (1979) Biophys. J. 26, 489–498
12 Lersch, W. and Michel-Beyerle, M.E. (1983) Chem. Phys. 78, 115–126
13 Ogrodnik, A., Lersch, W., Michel-Beyerle, M.E., Deisenhofer, J. and Michel, H. (1985) in Antennas and Reaction Centers of Photosynthetic Bacteria (Michel-Beyerle, M.E., ed.), pp. 198–206, Springer Verlag, Berlin
14 Krüger, H.-W. (1982) Thesis, Technische Universität München
15 Ferguson, R.C. and Marquardt, D.W. (1964) J. Chem. Phys. 41, 2087–2095
16 Ogrodnik, A., Krüger, H.-W., Orthuber, J., Haberkorn, R., Michel-Beyerle, M.E. and Scheer, H. (1982) Biophys. J. 39, 91–99
17 Norris, J.R., Bowman, M.K., Budil, D.E., Tang, J., Wraight, C.A. and Closs, G.L. (1982) Proc. Natl. Acad. Sci. USA 79, 5532–5536
18 Chidsey, C.E.D., Kirmaier, C., Holten, D. and Boxer, S.G. (1984) Biochim. Biophys. Acta 766, 424–437
19 Moehl, K.W., Lous, E.J. and Hoff, A.J. (1985) Chem. Phys. Lett. 121, 22–27
20 Lersch, W., Ogrodnik, A. and Michel-Beyerle, M.E. (1983) in Photochemistry and Photobiology (Zewail, A., ed.), Vol. 2, pp. 987–993, Harwood Academic Publishers, Chur
21 Deisenhofer, J. and Michel, H. (1985) in Antennas and Reaction Centers of Photosynthetic Bacteria (Michel-Beyerle, M.E., ed.), pp. 94–96, Springer Verlag, Berlin
22 Chidsey, C.E.D., Takiff, L., Goldstein, R.A. and Boxer, S.G. (1985) Proc. Natl. Acad. Sci. USA 82, 6850–6854
23 Lersch, W., Michel-Beyerle, M.E. and Knapp, E.W. (1985) J. Chem. Phys. 83, 2913–2922

24 Woodbury, N.W., Parson, W.W., Gunner, M.R., Prince, R.C. and Dutton, P.L. (1986) Biochim. Biophys. Acta 851, 6–22
25 Gunner, M.R., Robertson, D.E. and Dutton, P.L. (1986) J. Phys. Chem. 90, 3783–3795
26 Tang, J. and Norris, J.R. (1982) Chem. Phys. Lett. 92, 136–140
27 Lersch, W. (1982) Diplomarbeit, Technische Universität München
28 Lersch, W. and Michel-Beyerle, M.E. (1984) Chem. Phys. Lett. 107, 522–529